Modeling of Post-Myocardial Infarction and Its Solution Through Artificial Neural Network

Naheed Ali, Dr. Noor Badshah
Dept. of Basic Sciences and Islamiat University of Engineering and Technology Peshawar, Pakistan
*Correspondence: naheedali581@gmail.com, noorbadshah@uetpeshawar.edu.pk,
Citation | Ali. N, Badshah. N, "Modeling of Post-Myocardial Infarction and Its Solution Through Artificial Neural Network", IJIST, Special Issue pp 18-29, May 2024
Received | May 02, 2024, **Revised |** May 08, 2024, **Accepted |** May 14, 2024, **Published |** May 20, 2024.

Cardiovascular diseases, particularly myocardial infarction (MI) constitute a significant health concern globally. A myocardial infarction, which is commonly known as a heart attack, happens when a part of the heart muscle doesn't get enough blood because of a blockage. Studying MI is complex and it requires looking at it from different angles. In recent years the fusion of mathematical modeling and artificial intelligence (AI) techniques has emerged as a promising avenue for understanding the complexities associated with MI. The primary goal of this study is to provide an AI-based solution for a new nonlinear mathematical model related to myocardial infarction phenomena. To obtain the solution we will use a well-known deep learning technique, known as artificial neural networks (ANNs) with the combination of the optimization technique Levenberg-Marquardt back propagation (LMB). This combined method is referred to as ANNs-LMB. The results obtained from the model using ANNs-LMB are compared with a reference dataset constructed through the adaptive MATLAB solver ode45. The numerical performance is validated through a reduction in mean square error (MSE). The MSE is around 10^{-6} and the obtained results by ANNs-LMB almost overlapped with the reference dataset, which shows the accuracy and efficiency of the proposed methodology.
Keywords: Artificial Neural Network; Myocardial Infarction; Mathematical Modeling.

Introduction:

Myocardial Infarction, often referred to as a heart attack, stands as a significant contributor to morbidity and mortality globally. Myocardial infarction causes 17.1 million deaths per year throughout the world [1]. Based on the latest statistics from the World Health Organization (WHO) on the incidence of heart attacks in Pakistan, it was reported that 240,720 individuals lost their lives due to heart attacks in the year 2020. Smoking, inadequate physical activity, excessive body weight, elevated cholesterol levels, high blood pressure, and an unhealthy diet leading to elevated blood sugar are all factors that contribute to the risk of experiencing a myocardial infarction [2]. After a heart attack, the blockage in blood vessels stops oxygen and nutrients from reaching the heart muscle downstream. This causes damage to the heart, leading to a series of events like cell death, inflammation, and changes in the heart's structure, resulting in scars, stiffness, and altered function. People who've had a heart attack often face serious heart complications later on [3].

To respond to MI, the left ventricular (LV) of the heart will change its structural and functional behavior i.e. LV size, shape, and function called the remodeling of LV [4]. Because of the limited availability of experimental data and the biological complexity of LV remodeling, the understanding of the MI mechanism is a very complex process. By representing interaction of the factors such as blood flow, tissue oxygenation and cellular response through mathematical models can provide effective and valuable predictive capabilities. Previous studies [4][5][6], have explored the remodeling of left ventricular by using mathematical modeling. The approach employed in these articles involves using the numerical Runge-Kutta method with computer assistance to obtain the numerical solutions and collect various pieces of information. These investigations include exploring the important roles played by cytokines in the development of macrophages and other cells. Additionally, Zeigler et al. [7], has been investigated a mathematical model for fibrosis, using an ordinary differential equations (ODEs) framework to predict the behavior of collagen formation, breakdown, and aggregation. By using different assumptions, there exist some other papers [8][9], that include mathematical models to investigate the behavior of the heart after myocardial infarction, but all have some specific limitations. Agent-based models [10][11] have been employed to study tissue fibrosis, while biomechanical models [12][13] are also present in the literature. However, there is a scarcity of studies focusing on ODE models. Dealing with changes in the heart after myocardial infarction is always a challenge.

Various disciplines, including health, biology, physics, chemistry, civil and mechanical engineering, and economics, extensively use mathematical models [14][15][16][17][18][19]. In particular, there is a notable emphasis on combining these models with deep learning techniques, especially focusing on multilayer neural networks. In 2018, Side et al. [20] emphasized the crucial role of mathematical science in preventing the spread of illnesses. In addressing the spread of viruses, a mathematical model can be implemented, as in 2021 Umar et al. [21] highlighted the significant role of mathematics in exploring disease outbreaks, spread, and predictive patterns, particularly in the field of epidemiology. To obtain numerical outcomes for these models, stochastic solvers based on artificial neural networks along with optimization techniques are employed. Sabir et al. [22] present applications of artificial neural networks with the combination of Levenberg-Marquardt backpropagation for COVID-19 in 2022. In 2023 Haider et al. [23] proposed a system of ODEs for the study of hepatitis B virus (HBV) through deep learning techniques i.e. artificial neural network with the combination of Levenberg-Marquardt backpropagation. In this paper, we apply a deep learning methodology, specifically leveraging a widely recognized approach known as artificial neural networks, to infarction. In the diagram, cells are depicted by boxes with black color, while green boxes contain cytokines and specific proteins. Two types of arrows are used: black arrows signify the physical transfer of cells between groups, for instance, the transition of M_1 to M_2 macrophages and vice versa. On the other hand,

blue arrows denote interactions between distinct cell populations, like the release of cytokines by macrophages. The dotted black line represents the consumption rate of M_d by M_1.

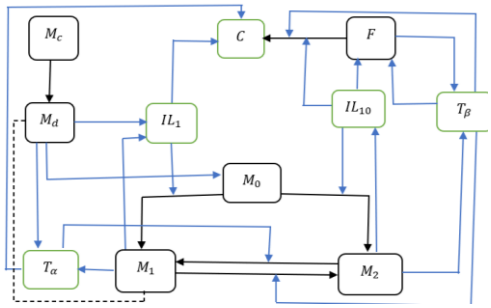

Figure 1: Diagram illustrating the cellular and molecular dynamics following a myocardial investigation of the phenomenon of myocardial infarction.

In the diagram, cells are depicted by boxes with black color, while green boxes contain cytokines and specific proteins. Two types of arrows are used: black arrows signify the physical transfer of cells between groups, for instance, the transition of M_1 to M_2 macrophages and vice versa. On the other hand, blue arrows denote interactions between distinct cell populations, like the release of cytokines by macrophages. The dotted black line represents the consumption rate of M_d by M_1.

The goal of this study is to introduce numerical simulations of the remodeling of MI through a nonlinear system of ODEs, including different compartments of the post-MI phenomenon. The solutions of the system are obtained using artificial neural networks methodology supported by an optimization technique called Levenberg-Marquardt backpropagation. Furthermore, an analysis of various components of ANNs-LMB is conducted to assess the proposed methodology's efficacy in achieving high accuracy and optimal performance. This method is suggested as an artificial intelligence-based approach for solving complex types of ODE systems with known initial conditions [24][25][26]. Some salient geographies of the designed study are given as follows:

- The MI mathematical model presented in this study is a modification of the mathematical model proposed by Lafci et al. [3]. We add two more cytokines: Transforming Growth Factor beta (T_β), and Tumor Necrosis Factor alpha (T_α), in the nonlinear system of ODEs proposed by Lafci et al. [3]. TGF-β is involved in the regulation of cell growth, differentiation, apoptosis, immune responses, and other cellular functions. It acts as a signaling molecule in various tissues and cell types, influencing both physiological and pathological processes [27], and is produced by alternatively activated macrophages (M_2) and fibroblasts (F). TNF-α is a cytokine involved in inflammation and immune system regulation. TNF-alpha is produced mainly by activated macrophages (M_1) and damaged cardiomyocytes (M_d) and can induce fever, inflammation, and cell death in certain tissues [28].
- Detailed descriptions of all compartments of the MI model are provided.
- The AI-based solutions of the model are performed by using a deep learning technique, ANNs-LMB in MATLAB.

Mathematical Model:

By incorporating T_β and T_α, and introducing some modifications to the mathematical model proposed in [3], our enhanced model is formulated as:

$$\frac{dM_c}{dt} = -k_1 M_c \quad (1)$$

$$\frac{dM_d}{dt} = k_1 M_c - k_2 M_1 M_d - \mu_1 M_d \quad (2)$$

$$\frac{dIL_1}{dt} = k_3 M_d + k_4 M_1 \frac{c_1}{c_1 + IL_{10}} - d_{IL_1} IL_1 \quad (3)$$

$$\frac{dIL_{10}}{dt} = k_5 M_2 \frac{c_2}{c_2 + IL_{10}} - d_{IL_{10}} IL_{10} \quad (4)$$

$$\frac{dM_0}{dt} = k_6 M_d - k_7 M_0 \frac{IL_1}{IL_1 + c_{IL_1}} - k_8 M_0 \frac{IL_{10}}{IL_{10} + c_{IL_{10}}} - \mu M_0 \quad (5)$$

$$\frac{dM_1}{dt} = k_7 M_0 \frac{IL_1}{IL_1 + c_{IL_1}} + \tau_1 M_2 \frac{T_\alpha}{T_\alpha + c_{T_\alpha}} - k_9 M_1 \frac{T_\beta}{T_\beta + c_{T_\beta}} - \mu M_1 \quad (6)$$

$$\frac{dM_2}{dt} = k_8 M_0 \frac{IL_{10}}{IL_{10} + c_{IL_{10}}} + k_9 M_1 \frac{T_\beta}{T_\beta + c_{T_\beta}} - \tau_1 M_2 \frac{T_\alpha}{T_\alpha + c_{T_\alpha}} - \mu M_2. \quad (7)$$

$$\frac{dC}{dt} = k_{10} F \frac{IL_{10}}{IL_{10} + c_3} + \alpha_1 F \frac{T_\beta}{T_\beta + \beta_1} - k_{11} C \frac{IL_1}{IL_1 + c_4} - \tau_2 C \frac{T_\alpha}{T_\alpha + c_4} - d_c C \quad (8)$$

$$\frac{dF}{dt} = k_{12} F \frac{IL_{10}}{IL_{10} + c_5} + \beta_2 F \frac{T_\beta}{T_\beta + \beta_1} - d_F F \quad (9)$$

$$\frac{dT_\beta}{dt} = \alpha_2 F + \alpha_3 M_2 - d_{T_\beta} T_\beta \quad (10)$$

$$\frac{dT_\alpha}{dt} = (\tau_3 M_1 + \tau_4 M_d) \frac{c_6}{c_6 + T_\beta} - d_{T_\alpha} T_\alpha \quad (11)$$

The model's parameters, along with their descriptions, values, and units are listed in Table 1. This mathematical model captures the cellular and molecular dynamics associated with MI. It is derived from the depicted interactions in Figure 1, which serves as a flow diagram illustrating the system dynamics after MI, specifically focusing on scenarios of post-MI without any medical interventions.

Equation 1 shows how the number of heart muscle cells (M_c) changes over time. Equation 2 explains how the number of damaged heart muscle cells (M_d) changes over time. It goes up as healthy cells M_c damage and decreases at a rate of k_2 and μ_1. Equation 3 illustrates how the concentration of interleukin 1 cytokines (IL_1) changes over time. These cytokines are released by both damaged heart muscle cells and a specific type of immune cells, classically activated macrophages (M_1). The impact of the inhibition by interleukin 10 cytokines (IL_{10}) is modeled as a decreasing function, where c_1 signifies the strength of inhibition. Equation 4 outlines the temporal evolution of IL_{10}. These cytokines are released by specific types of immune cells, alternatively activated macrophages (M_2). A decreasing function is used to depict the inhibition of IL_{10} by IL_1. Equation 5 explains how the quantity of monocytes (M_0) changes over time. It rises because of M_d and declines due to two factors: the differentiation of M_0 into M_1 and M_2, and a constant emigration rate. The transition of M_0 into M_1 is stimulated by interleukin 1, while the transition into M_2 is promoted by interleukin 10 cytokines. Equation 6 delineates how the density of M_1 changes over time. It increases when M_0 differentiates into M_1 and M_2 transferred into M_1 because of T_α, and decreases when M_1 transfer to M_2 by stimulation of T_β and emigration. Equation 7 portrays the temporal evolution of the density of M_2. It increases when M_0 activates M_2 and when M_1 shifts to M_2, and it decreases due to emigration. Equation 8 shows the variation in the density of collagen (C) over time. It increases as fibroblasts (F) produce collagen in response to stimulation by IL_{10} and T_β. On the other hand, it decreases due to degradation caused by the presence of IL_1, T_α and a constant decay rate represented by d_c. Equation 9 characterizes how the density of fibroblasts changes over time. It increases through stimulation by IL_{10} and T_β but decreases due to death or emigration, represented by the rate d_F. Equation 10 details the rate of change of transforming growth factor-β over time. It is secreted by both F and M_2. Equation 11 represents the change of T_α over time. It produces by M_1 and M_d with constant rates τ_3 and τ_4 respectively. A decreasing function is

used to represent the inhibition of T_α by T_β. In this equation d_{T_α} shows the decay rate of T_α by considering its half-life time.

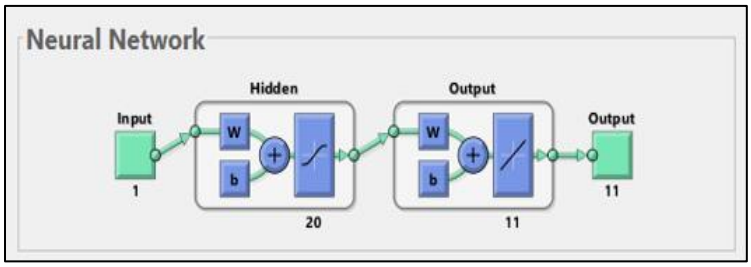

Figure 2: Designed A NNs-LMB

Table 1: MODEL'S PARAMETERS

Parameters	Description:	Values
k_1	Death rate of M_c	0.3
k_2	Rate at which M_d are consumed by M_1	0.003
k_3	Rate of Secretion of IL_1 by M_d	0.0004
k_4	Rate of Secretion of IL_1 by M_1	0.0005
k_5	Rate of Secretion of IL_{10} by M_2	0.0005
k_6	Rate of recruitment of M_0 based on M_d	0.4
k_7	Activation rate of IL_1 to activate M_1	0.7
k_8	Rate of activation of IL_{10} to activate M_2	0.3
k_9	Rate of transition from state M_1 to M_2	0.075
k_{10}	C production rate by F	26×10^5
k_{11}	Degradation rate of C by IL_1	0.0003
k_{12}	Fibroblasts growth rate	0.25
c_1	Effectiveness of IL_{10} inhibition on IL_1	2.5
c_2	Effectiveness of IL_1 inhibition on IL_{10}	10
c_3	Effectiveness of IL_{10} inhibition on F	5
c_4	Effectiveness of IL_1 and T_α on C	10
c_5	Impact of promoting of IL_{10} on F	2.5
c_6	Effectiveness of T_β inhibition on T_α	0.0007
τ_1	Transition rate of M_2 to M_1 because of T_α	0.7
τ_2	Degradation rate of C by T_α	0.0003
τ_3	Rate at which M_1 produces T_α	0.0007
τ_4	Rate at which M_d produces T_α	0.000005
α_1	Stimulation rate of transition of F to C by T_β	10
α_2	Secretion rate of T_β by F	0.0167
α_3	Rate at which M_2 produces T_β	0.0144
β_1	Effectiveness of T_β promotion on F	0.00316
β_2	Stimulation rate of T_β on F	0.03
c_{IL_1}	Impact of promoting of IL_1 on M_1	10
$c_{IL_{10}}$	Impact of promoting of IL_{10} on M_2	5
c_{T_β}	Effectiveness of T_β promotion on M_2	0.00316
c_{T_α}	Impact of promoting of T_α on M_1	10
d_{IL_1}	Decay rate of IL_1 considering its half-life time	0.2
$d_{IL_{10}}$	Decay rate of IL_{10} considering its half-life time	0.2

d_C	The decay rate of C by some enzymes	0.002
d_F	Emigration rate of F	0.02
d_{T_β}	Decay rate of T_β considering its half-life time	4.06
d_{T_α}	Decay rate of T_α considering its half-life time	0.5
μ	M_0, M_1 and M_2 emigration rate	0.2
μ_1	Removal rate of M_d	0.002

Methodology:

The two-step approach to the stochastic numerical procedure for the MI mathematical model is used. The first step involves offering comprehensive and detailed explanations of the computational stochastic numerical procedure, which is centered on ANNs-LMB. The second step encompasses the implementation procedures that bolster the stochastic numerical computation for the MI nonlinear mathematical model. The implementation of ANNs-LMB is employed to analyze and utilize the computational stochastic numerical outcomes of the mathematical model for myocardial infarction. We use MATLAB for the implementation of ANNs-LMB to obtain the results.

The "MATLAB" implementation follows a specific structure depicted in Figure 2, comprising a single input layer, hidden layers, and output layers. The configuration involves 20 hidden neurons, n-fold cross-validation, a log-sigmoid activation function, 20000 epochs, and the Levenberg-Marquardt optimization algorithm. It is important to highlight that the label data for input and targets are obtained from the standard numerical solution i.e. MATLAB solver command ode45.

Table 2: Model's Initial Conditions

Variables	Values	Units
$M_c(0)$	400	cells/mL
$M_d(0)$	0	cells/mL
$IL_1(0)$	0.00001	pg/mL
$IL_{10}(0)$	0.000001	pg/mL
$M_0(0)$	0.02	cells/mL
$M_1(0)$	0	cells/mL
$M_2(0)$	0	cells/mL
$C(0)$	839.5	pg/mL
$F(0)$	1	cells/mL
$T_\beta(0)$	0.054	pg/mL
$T_\alpha(0)$	0.00001	pg/mL

Numerical Simulations:

The parameters used in the numerical simulations are presented in Table 1, providing descriptions and values for each parameter. The initial values of all compartments used in the model are illustrated in Table 2. Numerical outcomes for the nonlinear dynamical model of myocardial infarction within the input range [0, 60] are obtained through the ANNs-LMB methodology. The results are generated by using MATLAB and depicted in Figures 3-6. The graphs illustrating calculated results for the MI mathematical model are presented in Figures 3-6. In particular,

In particular, Figure 3 offers insights into the performance, error histogram with 20 bins, and regressions of the applied methodology. Specifically, Figure 3(a) displays the calculated mean square error, measures for the best curves during training, validation, and testing with optimal performance achieved at epoch 20000, which is 2.6795×10^{-6}. These visual representations underscore the successful convergence and precision achieved by the used methodology. Moreover, in Figure 3(c), correlation measures are presented, highlighting the regression

performances. The correlation performances, expressed as the coefficient of determination (R^2 values), predominantly approach 1, underscoring the precision in solving the model. These plots encompass training, validation, testing and collectively indicating the accuracy of the scheme. Finally, fitting curves are depicted in Figure 4 to show the comparison between training, validation, and testing of the used methodology.

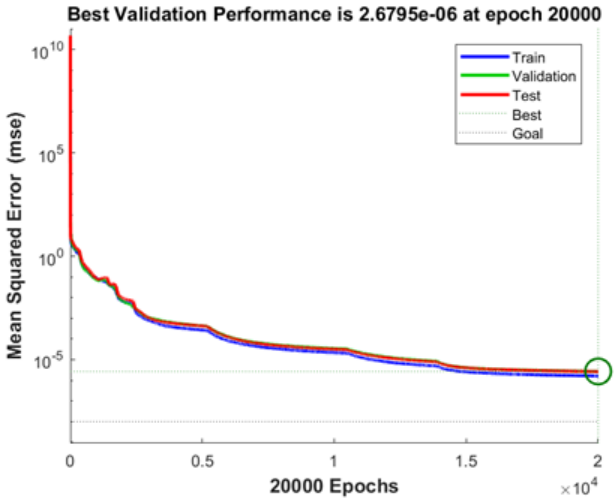

(a)

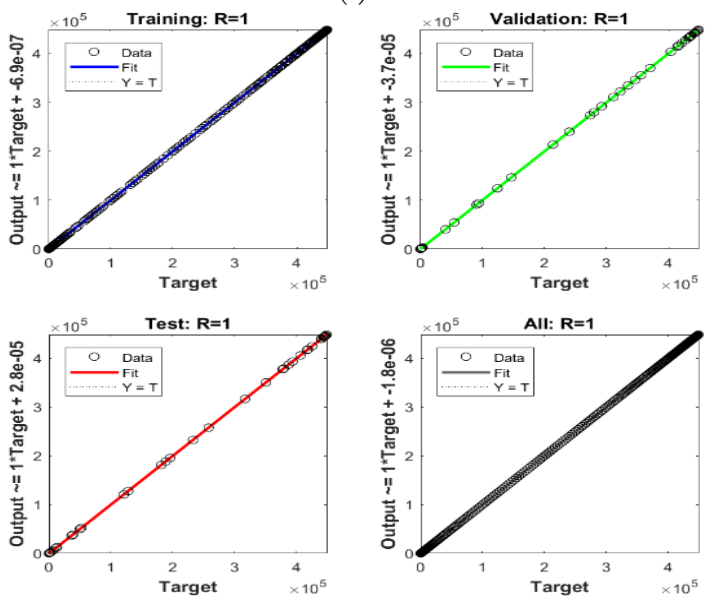

(b)

Figure 3: The performance of the used methodology ANNs-LMB to solve the MI mathematical model is presented in (a). Error histogram, and regression measure through ANNs-LMB are shown in (b) and (c) respectively.

Figures 5 and 6 display comparison plots of the solutions obtained by using the ANNs-LMB methodology and the true solutions (reference dataset constructed through MATLAB solver ode45) for the nonlinear dynamical system associated with myocardial infarction. Figure 5(a) compares the ANNs-LMB solution with the exact solution of the cardiomyocytes. We can observe that the solution obtained by ANNs-LMB and the exact solution are almost overlapped. Similarly, comparisons of dead cardiomyocytes, monocytes, macrophages, and fibroblasts are presented in Figure 5(b)-5(f). The comparison of cytokines and proteins after myocardial infarction is presented in Figure 6. These plots reveal a nearly perfect overlap between the exact solutions and those obtained by ANNs-LMB,

underscoring the precision and effectiveness of the designed ANNs-LMB in solving the nonlinear system of differential equations related to the phenomena of myocardial infarction.

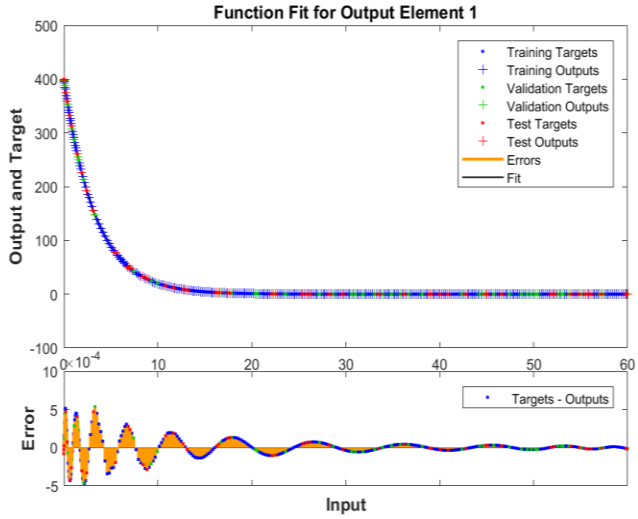

Figure 4: Function fit for output

Discussion:

A mathematical model is constructed to encompass critical interactions among cardiac cells, immune responses, and matrix proteins following myocardial infarction. Our model represents a notable improvement over earlier mathematical models, as highlighted in the work by Lafci et al. [3]. It stands out for considering significant biological factors, explicitly addressing the change of cardiomyocytes, the behavior of fibroblasts, and the deposition of fibrotic collagen in the context of post-myocardial infarction. Through numerical simulations, we tested the model's ability to describe events following a heart attack. The model's accurate predictability enhances our understanding of left ventricular remodeling after a heart attack. To derive solutions for the model, we used the deep learning strategy known as ANNs-LMB.

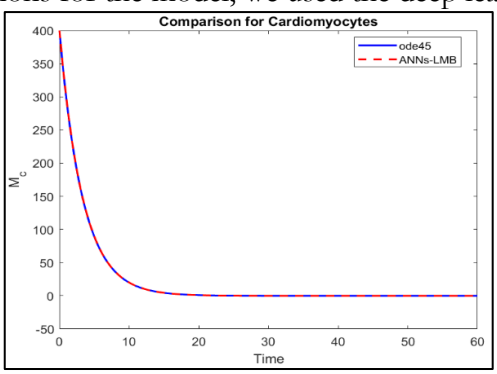

(a)

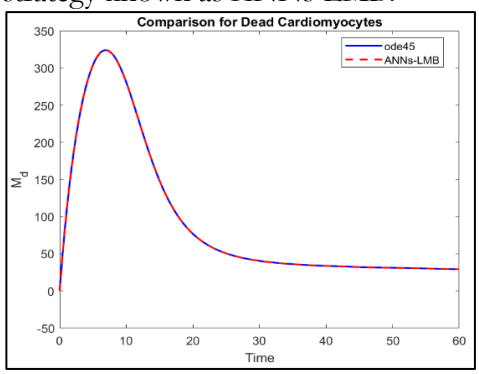

(b)

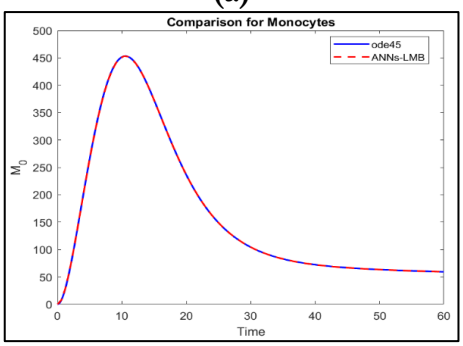

(c)

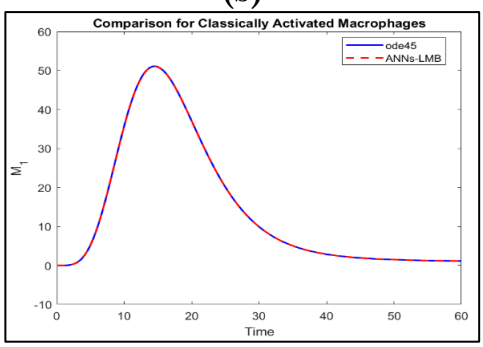

(d)

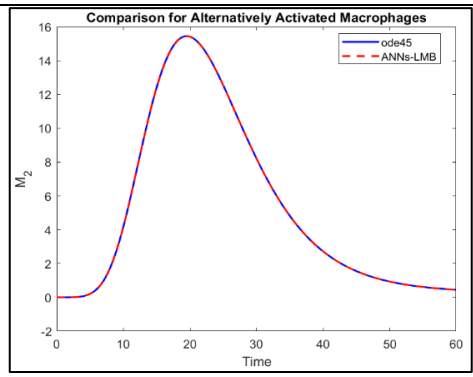

(e)

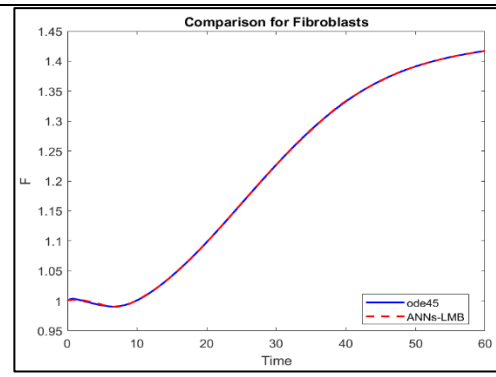

(f)

Figure 5: Dynamical behavior of cells after MI

Many papers on mathematical models lack visual representations, such as plots, that illustrate the evolution of various populations and species over time. While notable exceptions include the works of Jin et al. [4] and Wang et al. [5], Lafci et al.'s paper [3] stands out by providing insightful plots of evolution. To enhance understanding, we introduced changes to Lafci et al.'s model, particularly by adding two new compartments, TGF-β and TNF-α, and then solving the modified model by using a deep learning strategy, specifically ANNs-LMB.

Existing models related to MI, capture various aspects but often neglect key components. For example, Wang's model considers the monocytes and macrophage relationship, inhibitory and synthesizing bio factors, yet overlooks collagen, fibroblasts, and cardiomyocytes. Jin's model includes multiple elements but omits the behavior of cardiomyocytes. Zeigler et al. [7] primarily focus on fibroblast and collagen concentrations post-MI. Our study distinguishes itself by incorporating two additional compartments into the existing model proposed by Lafci et al., which plays a role in left ventricular remodeling after myocardial infarction. Furthermore, we obtained solutions for the myocardial infarction mathematical model by applying the deep learning strategy ANNs-LMB. Despite its thoroughness, a limitation stems from the lack of clinical data to derive certain unknown parameters. This model's limitation can be addressed in the future with more detailed data, allowing for a more precise representation of post-MI biological processes. Additionally, in this work, we used eleven compartments of the MI phenomena, a simplification compared to the real-world scenario. Future improvements may involve including more compartments to reduce this limitation.

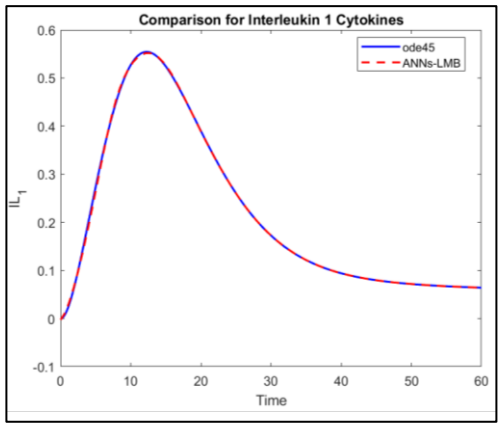

(a)

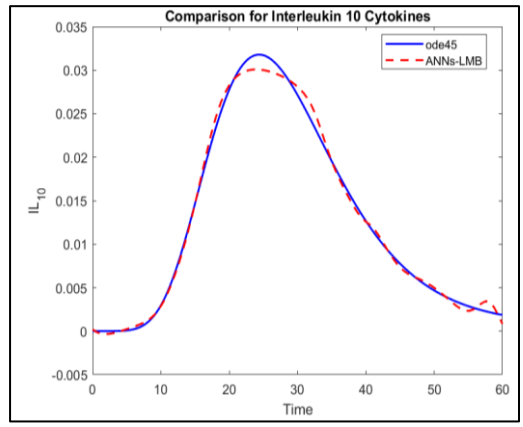

(b)

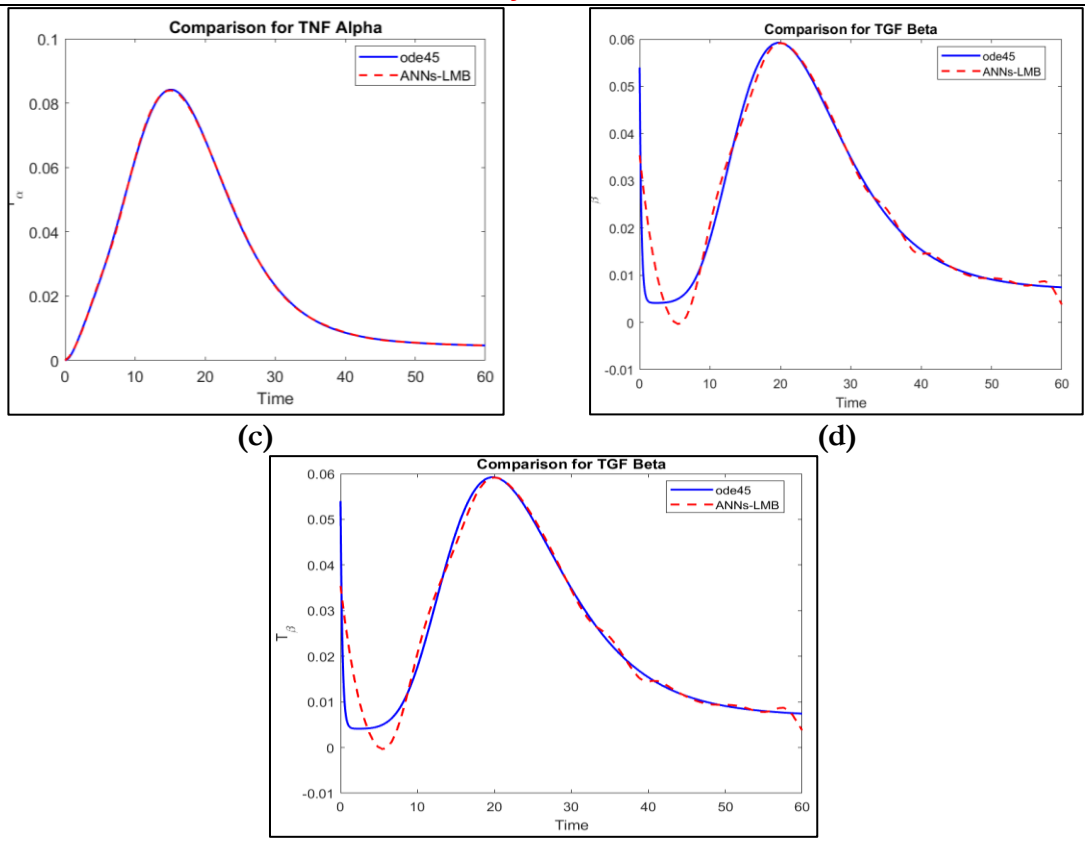

Figure 6: Dynamical behavior of cytokines and proteins after MI.

Conclusions:

The objective of the current study is to apply deep learning strategies for the investigation of myocardial infarction through mathematical modeling. Several parameters in the mathematical model proposed by Lafci et al., for myocardial infarction are modified. The primary alteration involves the addition of two more compartments, namely Transforming Growth Factor beta and Tumor Necrosis Factor-alpha. Results of the nonlinear dynamical MI mathematical model are obtained by using a deep learning technique ANNs-LMB. The mathematical model is dependent on eleven dimensions.

Validation, testing, and training processes are conducted utilizing ANNs-LMB for the MI mathematical model. The numerical solutions derived from the model are compared with a reference dataset constructed through MATLAB. The outcomes demonstrate a notable overlapping with the reference dataset, underscoring the accuracy of the used methodology. Additionally, the results are further validated through the reduction of MSE. To evaluate the precision, reliability, and efficiency of the approach, various analyses, including MSE, error histograms, and regressions are used in this study.

References:

[1] T. I. Siddiqui, A. K. K. S., and D. K. Dikshit, "Platelets and Atherothrombosis: Causes, Targets and Treatments for Thrombosis," Curr. Med. Chem., vol. 20, no. 22, pp. 2779–2797, Jun. 2013, doi: 10.2174/09298673113202200004.

[2] R. Hajar, "Risk Factors for Coronary Artery Disease: Historical Perspectives," Heart Views, vol. 18, no. 3, p. 109, 2017, doi: 10.4103/HEARTVIEWS.HEARTVIEWS_106_17.

[3] M. Lafci Büyükkahraman, G. K. Sabine, H. V. Kojouharov, B. M. Chen-Charpentier, S. R. McMahan, and J. Liao, "Using models to advance medicine: mathematical modeling

of post-myocardial infarction left ventricular remodeling," Comput. Methods Biomech. Biomed. Engin., vol. 25, no. 3, pp. 298–307, 2022, doi: 10.1080/10255842.2021.1953487.

[4] Y. F. Jin, H. C. Han, J. Berger, Q. Dai, and M. L. Lindsey, "Combining experimental and mathematical modeling to reveal mechanisms of macrophage-dependent left ventricular remodeling," BMC Syst. Biol., vol. 5, no. 1, pp. 1–14, May 2011, doi: 10.1186/1752-0509-5-60/FIGURES/6.

[5] Y. Wang et al., "Mathematical modeling and stability analysis of macrophage activation in left ventricular remodeling post-myocardial infarction.," BMC Genomics, vol. 13 Suppl 6, no. 6, pp. 1–8, Oct. 2012, doi: 10.1186/1471-2164-13-S6-S21/FIGURES/4.

[6] U. Pagalay, L. Handayani, and A. Azzam, "Dynamics of Macrofages and Cytokines after Myocardial Infarction," Jun. 2019, doi: 10.4108/EAI.2-5-2019.2284674.

[7] A. C. Zeigler, A. R. Nelson, A. S. Chandrabhatla, O. Brazhkina, J. W. Holmes, and J. J. Saucerman, "Computational Model Predicts Paracrine and Intracellular Drivers of Fibroblast Phenotype After Myocardial Infarction," bioRxiv, p. 840017, Nov. 2019, doi: 10.1101/840017.

[8] L. C. Lee, G. S. Kassab, and J. M. Guccione, "Mathematical modeling of cardiac growth and remodeling," Wiley Interdiscip. Rev. Syst. Biol. Med., vol. 8, no. 3, pp. 211–226, May 2016, doi: 10.1002/WSBM.1330.

[9] N. Moise and A. Friedman, "A mathematical model of immunomodulatory treatment in myocardial infarction," J. Theor. Biol., vol. 544, p. 111122, Jul. 2022, doi: 10.1016/J.JTBI.2022.111122.

[10] A. D. Rouillard and J. W. Holmes, "Mechanical regulation of fibroblast migration and collagen remodelling in healing myocardial infarcts," J. Physiol., vol. 590, no. 18, pp. 4585–4602, Sep. 2012, doi: 10.1113/JPHYSIOL.2012.229484.

[11] S. M. Rikard et al., "Multiscale Coupling of an Agent-Based Model of Tissue Fibrosis and a Logic-Based Model of Intracellular Signaling," Front. Physiol., vol. 10, p. 479813, Dec. 2019, doi: 10.3389/FPHYS.2019.01481/BIBTEX.

[12] P. Sáez and E. Kuhl, "Computational modeling of acute myocardial infarction," Comput. Methods Biomech. Biomed. Engin., vol. 19, no. 10, pp. 1107–1115, Jul. 2016, doi: 10.1080/10255842.2015.1105965.

[13] E. Cutrì, A. Meoli, G. Dubini, F. Migliavacca, T. Y. Hsia, and G. Pennati, "Patient-specific biomechanical model of hypoplastic left heart to predict post-operative cardio-circulatory behaviour," Med. Eng. Phys., vol. 47, pp. 85–92, Sep. 2017, doi: 10.1016/J.MEDENGPHY.2017.06.024.

[14] M. Lo Schiavo, B. Prinari, J. A. Gronski, and A. V. Serio, "An artificial neural network approach for modeling the ward atmosphere in a medical unit," Math. Comput. Simul., vol. 116, pp. 44–58, Oct. 2015, doi: 10.1016/J.MATCOM.2015.04.006.

[15] J. L. G. Guirao, "On the stochastic observation for the nonlinear system of the emigration and migration effects via artificial neural networks," Int. J. Math. Comput. Eng., vol. 1, no. 2, pp. 177–186, Dec. 2023, doi: 10.2478/IJMCE-2023-0014.

[16] M. Shoaib, R. Kainat, M. Ijaz Khan, B. C. Prasanna Kumara, R. Naveen Kumar, and M. A. Zahoor Raja, "Darcy-Forchheimer entropy based hybrid nanofluid flow over a stretchable surface: intelligent computing approach," Waves in Random and Complex Media, Sep. 2022, doi: 10.1080/17455030.2022.2122627.

[17] Z. Sabir, R. Sadat, M. R. Ali, S. Ben Said, and M. Azhar, "A numerical performance of the novel fractional water pollution model through the Levenberg-Marquardt backpropagation method," Arab. J. Chem., vol. 16, no. 2, p. 104493, Feb. 2023, doi: 10.1016/J.ARABJC.2022.104493.

[18] T. Botmart, Z. Sabir, M. A. Z. Raja, W. weera, R. Sadat, and M. R. Ali, "Stochastic procedures to solve the nonlinear mass and heat transfer model of Williamson nanofluid past over a stretching sheet," Ann. Nucl. Energy, vol. 181, p. 109564, Feb. 2023, doi: 10.1016/J.ANUCENE.2022.109564.

[19] W. Weera et al., "Fractional Order Environmental and Economic Model Investigations Using Artificial Neural Network," Comput. Mater. Contin., vol. 74, no. 1, pp. 1735–1748, Sep. 2022, doi: 10.32604/CMC.2023.032950.

[20] "Stability Analysis Susceptible, Exposed, Infected, Recovered (SEIR) Model for Spread Model for Spread of Dengue Fever in Medan", [Online]. Available: https://iopscience.iop.org/article/10.1088/1742-6596/954/1/012018

[21] M. Umar et al., "Numerical Investigations through ANNs for Solving COVID-19 Model," Int. J. Environ. Res. Public Heal. 2021, Vol. 18, Page 12192, vol. 18, no. 22, p. 12192, Nov. 2021, doi: 10.3390/IJERPH182212192.

[22] Z. Sabir, M. A. Z. Raja, S. E. Alhazmi, M. Gupta, A. Arbi, and I. A. Baba, "Applications of artificial neural network to solve the nonlinear COVID-19 mathematical model based on the dynamics of SIQ," J. Taibah Univ. Sci., vol. 16, no. 1, pp. 874–884, Dec. 2022, doi: 10.1080/16583655.2022.2119734.

[23] Q. Haider, A. Hassan, and S. M. Eldin, "Artificial neural network scheme to solve the hepatitis B virus model," Front. Appl. Math. Stat., vol. 9, p. 1072447, Mar. 2023, doi: 10.3389/FAMS.2023.1072447/BIBTEX.

[24] Z. Sabir et al., "Artificial neural network scheme to solve the nonlinear influenza disease model," Biomed. Signal Process. Control, vol. 75, p. 103594, May 2022, doi: 10.1016/J.BSPC.2022.103594.

[25] S. Mall and S. Chakraverty, "Comparison of Artificial Neural Network Architecture in Solving Ordinary Differential Equations," Adv. Artif. Neural Syst., vol. 2013, pp. 1–12, Dec. 2013, doi: 10.1155/2013/181895.

[26] Y. Wen, T. Chaolu, and X. Wang, "Solving the initial value problem of ordinary differential equations by Lie group based neural network method," PLoS One, vol. 17, no. 4, p. e0265992, Apr. 2022, doi: 10.1371/JOURNAL.PONE.0265992.

[27] M. Bujak and N. G. Frangogiannis, "The role of TGF-β signaling in myocardial infarction and cardiac remodeling," Cardiovasc. Res., vol. 74, no. 2, pp. 184–195, May 2007, doi: 10.1016/J.CARDIORES.2006.10.002/2/74-2-184-FIG4.GIF.

[28] D. I. Jang et al., "The Role of Tumor Necrosis Factor Alpha (TNF-α) in Autoimmune Disease and Current TNF-α Inhibitors in Therapeutics," Int. J. Mol. Sci. 2021, Vol. 22, Page 2719, vol. 22, no. 5, p. 2719, Mar. 2021, doi: 10.3390/IJMS22052719.